

Article

Spongin-Based Scaffolds from *Hippospongia communis* Demosponge as an Effective Support for Lipase Immobilization

Jakub Zdarta ^{1,*}, Małgorzata Norman ¹, Wojciech Smulek ¹, Dariusz Moszyński ², Ewa Kaczorek ¹, Allison L. Stelling ³, Hermann Ehrlich ⁴ and Teofil Jesionowski ^{1,*}

¹ Institute of Chemical Technology and Engineering, Faculty of Chemical Technology, Poznan University of Technology, Berdychowo 4, PL-60965 Poznan, Poland; malgorzata.norman@hotmail.com (M.N.); wojciech.smulek@doctorate.put.poznan.pl (W.S.); ewa.kaczorek@put.poznan.pl (E.K.)

² Institute of Chemical and Environment Engineering, Faculty of Chemical Technology and Engineering, West Pomeranian University of Technology, Szczecin, Pulaskiego 10, PL-70322 Szczecin, Poland; dmoszynski@zut.edu.pl

³ Department of Biochemistry, Duke University, 307 Research Drive, Durham, NC 27710, USA; allison.stelling@duke.edu

⁴ Institute of Experimental Physics, TU Bergakademie Freiberg, Leipziger Str. 23, Freiberg 09599, Germany; hermann.ehrlich@physik.tu-freiberg.de

* Correspondence: jakub_zdarta@wp.pl (J.Z.); Teofil.Jesionowski@put.poznan.pl (T.J.); Tel.: +48-61-665-3747 (J.Z.); +48-61-665-3720 (T.J.)

Academic Editor: David D. Boehr

Received: 31 March 2017; Accepted: 5 May 2017; Published: 10 May 2017

Abstract: The main purpose of the study was to achieve effective immobilization of lipase B from *Candida antarctica* (CALB) onto 3D spongin-based scaffolds from *Hippospongia communis* marine demosponge for rapeseed oil transesterification. Successful immobilization onto the marine sponge skeleton was confirmed for the first time. Lipase B-containing biocatalytic system exhibited the highest catalytic activity retention (89%) after 60 min of immobilization at pH 7 and temperature of 4 °C. Immobilization was found to improve the thermal and chemical stability compared to free lipase, and retain over 80% of its initial catalytic activity over a wide range of temperature (30–60 °C) and pH (6–9). Additionally, immobilized lipase has good storage stability and retains over 70% of its initial activity even after catalyzing of 25 reaction cycles. The obtained product was used in a transesterification reaction of rapeseed oil with methanol and proved to be an efficient biocatalyst for biofuel production. The highest conversion value and fatty acids methyl esters (FAME) concentration were observed after a process conducted at 40 °C and pH 10. The possible mechanism of interaction between the enzyme and the spongin-based support is proposed and discussed.

Keywords: *Hippospongia communis* scaffolds; lipase B from *Candida antarctica*; lipase immobilization; immobilized lipase stability and reusability; rapeseed oil transesterification

1. Introduction

The industrial use of enzymes has continued to grow over recent years, but their utilization in many commercial applications is limited by rapid loss of catalytic activity, affected by even slight changes to their optimal operational conditions [1]. Immobilization is commonly known as one of the best methods to enhance catalytic properties as well as stability and resistance against inhibitors of biocatalysts [2–5]. However, the greatest advantage of this process is that it allows catalysts to be obtained in heterogeneous form. Moreover, immobilization helps to overcome enzyme aggregation, typically observed for free enzymes in solution [6].

Generally, attachment of the proteins to the solid support takes place via physical interactions as well as the formation of covalent bonds [7]. Methods based on the adsorption of biocatalysts on the matrix surface are simple and the most widely applied. This might be explained by the fact that there are insignificant conformational changes in the structure of the enzyme and its active sites, thus catalytic activity is maintained at a high level [8,9]. An additional benefit of this method is that the matrix may be formed by a very broad group of materials of various origins, ranging from inorganic compounds via synthetic up to organic materials obtained from natural sources [10,11]. This last group of compounds is particularly interesting because of their renewability. They include, for instance, collagens, keratins, chitin, chitosan and cellulose [12]. Furthermore, since 1970, there has been an increase in the use of natural marine sponges as matrices for immobilization of diverse enzymes [13–15].

The increasing use of these materials is linked to their three-dimensional open fibrous network built of microfibers of various diameters, depending on the type of sponge [16]. This feature of their structure allows easy infiltration of the reaction substrates to the active sites of the immobilized enzyme, and thus helps to avoid diffusional limitations [17]. A promising support, which meets the above criteria, is found in diverse marine keratan sponges of the *Dictyoceratida* order, which are cultivated worldwide under marine ranching conditions. One of the typical representatives of this order is *Hippospongia communis* whose skeleton consists of mineral-free fibrous spongin. This structural, halogenated keratin-like protein [18] is also well-known in applications for tissue engineering due to its biocompatibility and good mechanical resistance [19–22].

Spongin shows excellent sorption properties [23] and additionally increases the affinity of the material to diverse enzymes and helps to create strong and stable interactions [15].

Lipases (EC 3.1.1.3) are among the most commonly used biocatalysts, because of their wide application in esterification, transesterification and hydrolysis processes for a variety of chemical compounds. The high catalytic activity of the enzymes in such reactions is directly related to their chemical structure and the geometries of their active sites. Catalytic sites of these enzymes are made up of a three residues (His25T, Asp203 and Ser144) as reported by Derewenda et al. [24]. This triad is known from the very similar structure of the triad found in the serine proteinases. This type of the composition of the lipase active caused that lipases possess a unique and important property called interfacial activation [25,26]. This phenomenon thought to arise from the conformational changes occurring in the active site of the peptide under the influence of the hydrophobic interface. In these conditions, the oligopeptide lid of the active site opens, making it accessible to the reaction substrates [27,28]. Various types of lipases are known from their commercial use in biodiesel production, where they enable a high level of substrate conversion to be attained. A number of studies have pointed to the application of these enzymes, in immobilized forms, in the transformation of vegetable oils with short-chain alcohols. Results previously obtained have shown that transesterification can be carried out with satisfactory yield and high conversion rate of triglycerides under mild conditions and with short reaction times [29–31].

The present work, to the best of our knowledge, describes for the first time the use of marine sponges of the species *Hippospongia communis* as a natural and renewable source of spongin-based matrix as a stable and suitable scaffold for the immobilization of *Candida antarctica* lipase B (CALB). The products obtained, following immobilization, possess good operational stability and their chemical structure facilitates the creation of stable interactions between enzyme and matrix. Use of the immobilized lipase in the transesterification reaction of rapeseed oil with methanol has proved that they can fulfill an important role in these processes and enable the production of fatty acids methyl esters (FAME), an important material for the production of eco-friendly fuel—biodiesel. This is of great importance from the point of view of potential applications because lipase-spongin scaffold systems could be used on an industrial scale as efficient and environmentally friendly biocatalysts.

2. Results and Discussion

2.1. SEM and Digital Microscopy

The SEM images (Figure 1a–d) and digital light microscopy images (Figure 1e,f) show the spongin-based scaffolds isolated from *H. communis* skeletons before and after lipase immobilization, at different magnifications.

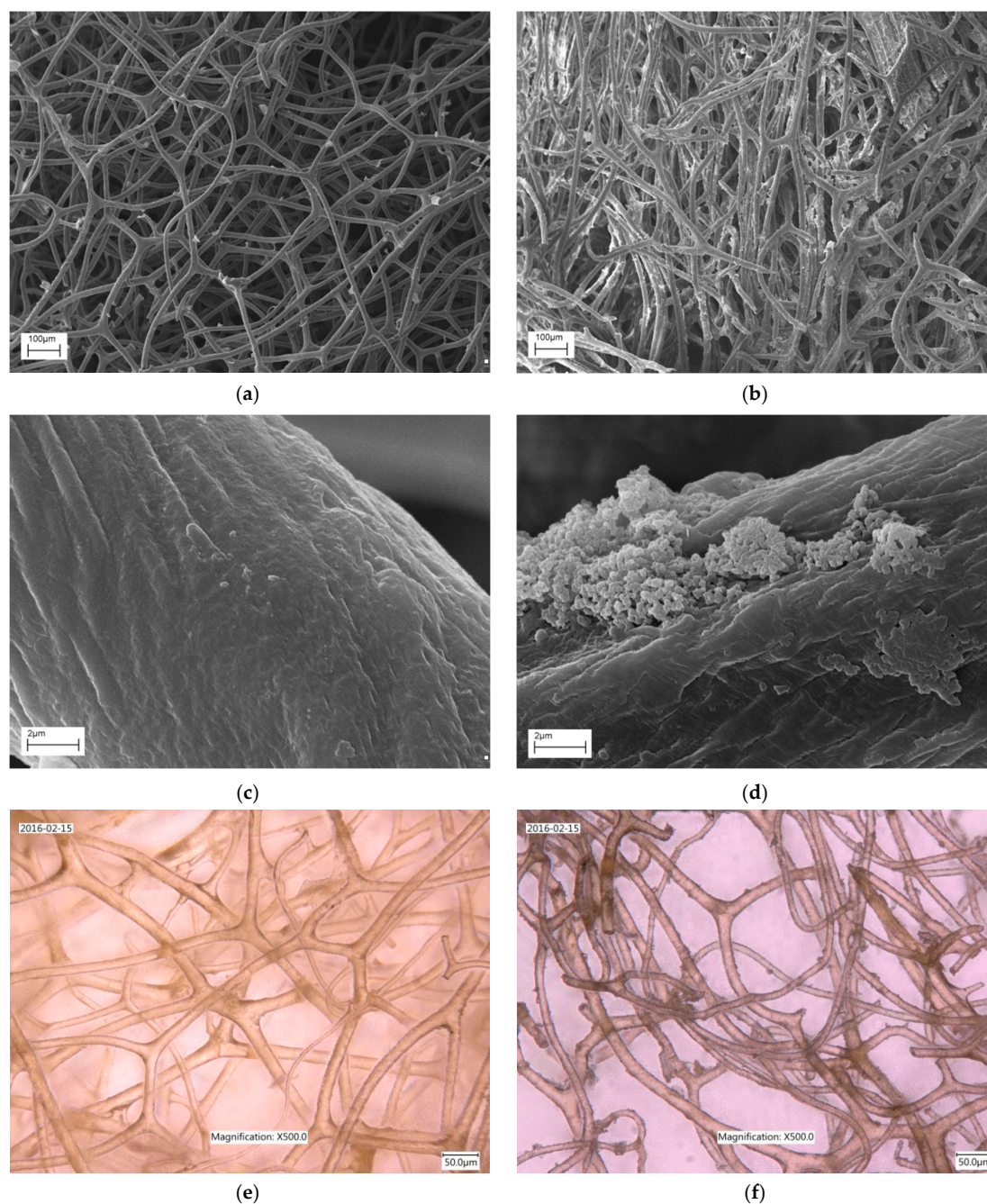


Figure 1. Scanning electron microscopy (SEM) images of spongin-based scaffold without (a,c) and with immobilized lipase B from *C. antarctica* (b,d) at various magnifications. The digital microscope images of the scaffolds prior and after enzyme immobilization are represented as (e,f), respectively.

The marine keratanos demosponges exhibit a three-dimensional open network structure built from similar, branched spongin fibers with a slightly corrugated surface at a diameter of 20 μm [32,33].

SEM images taken after enzyme immobilization (process parameters: 2 h process duration, 4 °C, pH 7) confirmed the successful deposition of the lipase by the presence of enzyme aggregates on the surface of the spongin fibers, as mentioned previously [34]. These results are confirmed by observations from digital microscopy (Figure 1e,f). It should also be noted that sponge's fibers are coated by the enzyme particles that formed aggregates of various shapes and sizes.

2.2. FTIR Spectroscopy

The spongin-based scaffolds, free CALB and obtained biocatalytic system were analyzed by FTIR. The spectra obtained for these materials are presented in Figure 2.

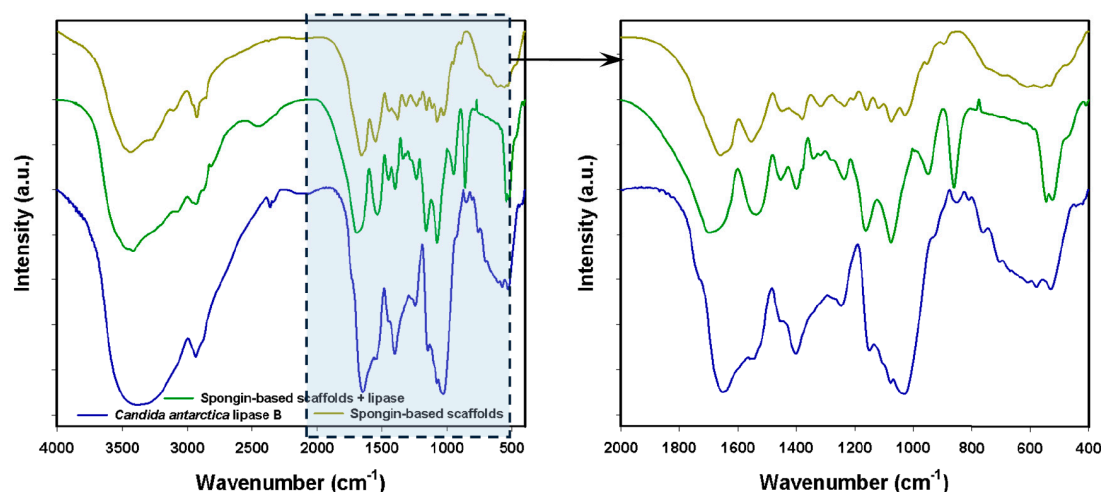


Figure 2. FTIR spectra of *C. antarctica* lipase B, spongin-based scaffolds and obtained biocatalytic system (process carried out at pH 7, $T = 4$ °C, $t = 60$ min, $C_{enz} = 3$ mg/mL).

Detailed data on the most important signals present on the FTIR spectra, confirming effective enzyme immobilization, are given in Table 1.

Table 1. Characteristic wavenumbers (cm^{-1}) of the signals present on the FTIR spectra for *C. antarctica* lipase B, spongin-based scaffolds and produced biocatalytic system.

<i>Candida antarctica</i> Lipase B	Spongin	Product Following Immobilization	Vibrational Assignment
3480	3435	3445	–OH stretching
3325	3292	3295	–NH stretching
2937	2927	2929	C–H stretching
1643	1647	1655	–NH deformational (amide I)
1542	1546	1538	–NH stretching (amide II)
1394	1375	1390	C–OH bending
1256	1243	1240	C–N stretching (amide III)
1026	1154, 1073	1150, 1065	C–O–C stretching
815	-	820	–NH ₂ deformational
645–535	640–530	580–530	C–C bending

The FTIR spectrum of the biocatalytic system (Figure 2) contains signals characteristic for the functional groups of the support and lipase. Most important is the presence of the peaks at wavenumbers 1655, 1538 and 1256 cm^{-1} , related, respectively, to the vibrations of amide I, amide II and amide III bonds in the structure of the enzyme. The existence of these signals is asserted to be evidence of effective protein immobilization, as reported by Wong et al. [35]. Moreover, changes in the intensity of signals generated by particular functional groups, mainly –OH and –NH, indirectly confirmed successful immobilization of the lipase on the spongin-based scaffolds.

Additionally, slight changes in the maximal wavenumbers of the signals on the spectrum of the obtained biocatalytic system were noted. This may indicate that enzyme particles are attached to the surface of spongin via hydrogen bonds [36].

2.3. ^{13}C CP MAS NMR Spectra

On the spongin-based scaffold spectrum (Figure 3a), the signals in the low-field part (20–70 ppm) could be assigned to aliphatic carbons and several functional groups characteristic for the spongin structure: C–NH₂, C–OH, C–OR or C–COOR. Peaks at 92.2 and 172.1 ppm indicate the presence of aromatic carbons and carboxyl or ester groups (R–COOH or R–COOR), respectively.

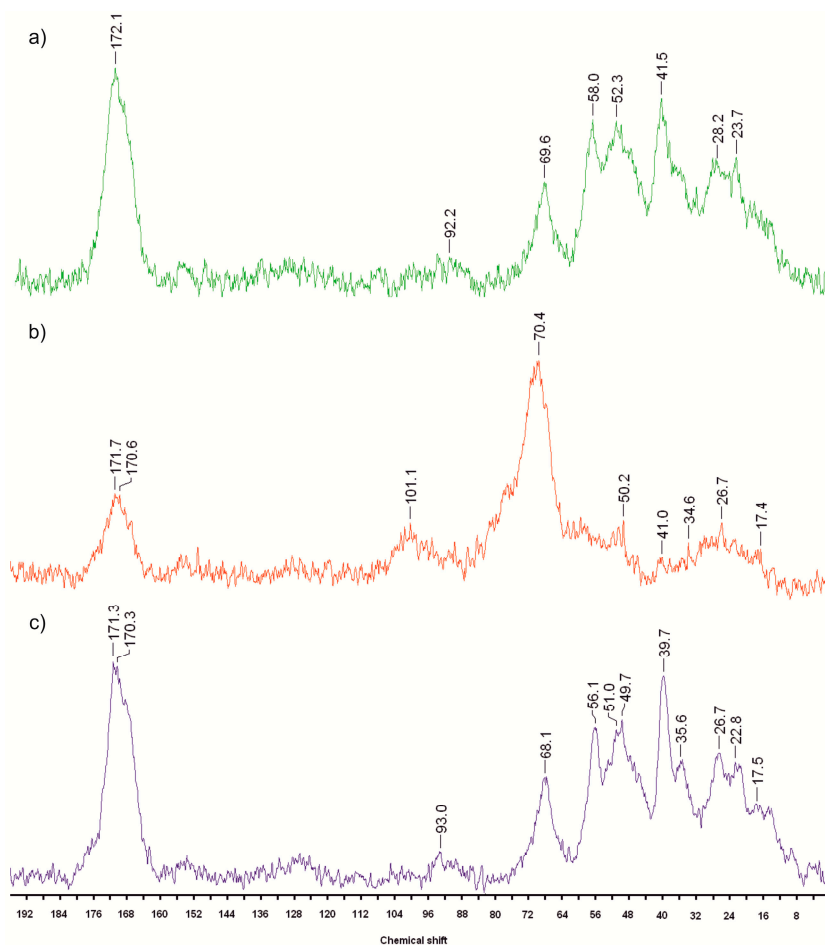


Figure 3. Solid-state Cross-Polarization Magic Angle Spinning Carbon-13 Nuclear Magnetic Resonance (^{13}C CP MAS NMR) spectra of: spongin-based scaffold (a); CALB (b); and the product following immobilization (c) (process parameters: pH 7, $T = 4\text{ }^\circ\text{C}$, $t = 60\text{ min}$, $C_{\text{enz}} = 3\text{ mg/mL}$).

The ^{13}C CP MAS NMR spectrum of lipase B from *C. antarctica* is a typical protein spectrum with broad resonance signals, characteristic for large molecules. Specific assignments are not possible because of the low resolution of the spectrum. Nevertheless, according to Beinert et al. [37], signals below 50 ppm are typical for aliphatic carbons, and above 100 ppm for aromatic carbons. The band at 70.4 ppm corresponds to carbon connected to oxygen, while the peaks at 170.6 and 171.7 ppm are related to the presence of carbonyl groups in the structure of CALB [38].

In the spectrum of the obtained biocatalytic system, no significant changes are observed. This might be explained by the similar chemical structure of the spongin that built the sponge skeleton and the lipase. However, a low-frequency shift and signal splitting are observed. These changes

are associated with changes in the chemical environment of selected carbon atoms caused by the immobilization process, related to the creation of new interactions (hydrogen bonds) between the enzyme and the support.

2.4. XPS Analysis

The surface composition of the *C. antarctica* lipase B, spongin-based scaffolds and obtained biocatalytic system was examined by means of X-ray photoelectron spectroscopy (XPS). The surface of all samples contains carbon, oxygen and nitrogen. Traces of calcium were identified on the surface of both samples based on sponges, and silicon only in the sample of unmodified sponges. The presence of these elements in low amounts is ascribed to the mineral skeletons of the sponges. Additionally, phosphorus and sodium XPS signals were observed in the spectrum of the immobilized lipase. The origin of these two elements is the phosphate buffer used during the preparation procedure. The elemental surface composition is calculated with the use of peak area intensities using the sensitivity factor approach, and is given in Table 2.

Table 2. Elemental composition of the surface of *C. antarctica* lipase, spongin-based scaffolds and produced biocatalytic system (process parameters: pH 7, $T = 4\text{ }^{\circ}\text{C}$, $t = 60\text{ min}$, $C_{enz} = 3\text{ mg/mL}$).

Sample Name	Atomic %							Ratio of	
	C	O	N	Ca	Si	Na	P	N/C	O/C
<i>C. antarctica</i> lipase B	58.2	30.7	11.1	-	-	-	-	0.19	0.53
Spongin-based scaffolds	73.4	17.4	7.3	0.6	1.3	-	-	0.10	0.24
Spongin-based scaffolds + CALB	53.9	31.7	9.7	0.8	-	1.3	2.6	0.18	0.59

The elemental composition of the lipase reported by Tomizuka et al. [39] expressed as a C/O/N molar ratio is 61:25:14. The C/O/N molar ratio observed by XPS in the present study is 58:31:11. This shows that the surface analysis is in relatively good agreement with the chemical analysis of this enzyme. The surface composition of spongin fibers expressed as a C/O/N molar ratio is 75:18:7 (calcium and silicon signals were excluded from the calculation). This differs substantially from the C/O/N molar ratio of the lipase, mostly in view of the much higher content of carbon. Both samples are bio-organic systems, and as such may vary significantly in chemical composition. The elemental composition of the obtained biocatalytic system expressed as a C/O/N molar ratio is 56:33:10 (calcium, sodium and phosphorus signals were excluded from the calculation). These figures, within the boundaries of experimental error, correspond well with the ratio observed for pure lipase. The similarity of the C/O/N molar ratios for lipase and obtained biocatalytic system is therefore considered an indicator of successful enzyme immobilization.

Additional insight into the chemical composition of the surface of the examined materials may be given by analysis of the XPS C 1s peak. Since bio-organic specimens are chemically very complicated systems, the decomposition of the XPS spectrum can generate ambiguous results. Therefore, in the present study, the reasoning is mostly based on the changes in the XPS spectra envelope. The C 1s lines coming from *C. antarctica* lipase B, spongin-based scaffolds and produced biocatalytic system are shown superimposed in Figure 4. The binding energy regions characteristic for carbon-carbon bonds (C–C), hydroxyl or amino groups (C–O/C–N) and carboxylic groups or peptide bonds (CO(N)) are depicted above the spectrum.

The maximum of the C 1s line coming from lipase at a binding energy of 285.8 eV. Organic substances in which C–C bonds prevail are characterized by an XPS C 1s line with the maximum located in the region around 285 eV. The prominent shift of the maximum observed for lipase indicates that the contents of carbon-oxygen or carbon-nitrogen bonds are significant in that substance. Since lipase is a protein it contains a considerable number of amino groups, which give rise to the carbon bindings in the region around 286 eV. Moreover, there is an evident shoulder on the

high-energy side of the spectrum at a binding energy of about 288 eV. This region is characteristic for the peptide bonds present in the lipase.

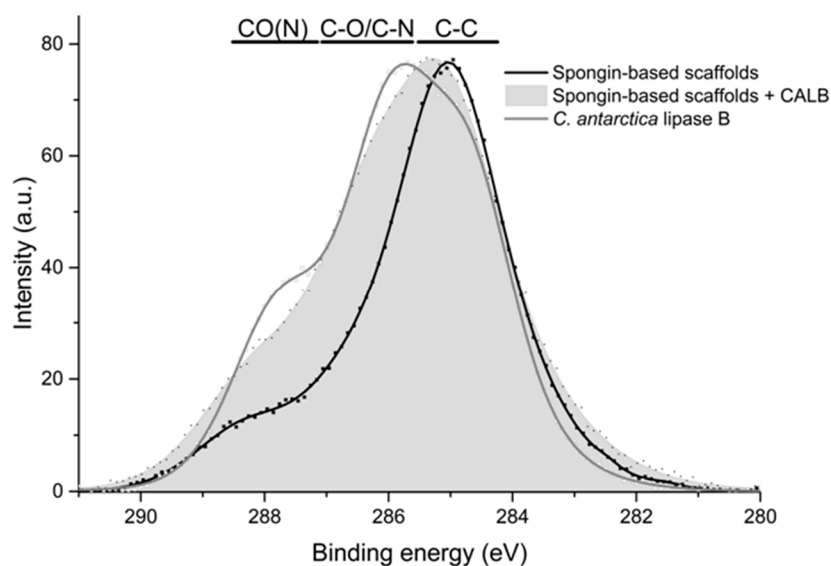


Figure 4. X-ray photoelectron spectroscopy (XPS) C 1s spectra for *C. antarctica* lipase B, spongin-based scaffolds and the product after immobilization.

The envelope of the C 1s spectrum acquired for spongin-based scaffolds differs notably from the spectrum of lipase. The maximum is located at a binding energy of 285.0 eV, and the width of the peak is smaller than observed for lipase. This position indicates that the surface of the spongin contains mostly C–C bonds. There is also a small shoulder at about 288 eV, which can be attributed to the presence of carboxylic bonds. Since the surface concentration of nitrogen in the spongin is still relatively high (7.3 at. %) this region may also contain an XPS signal coming from peptide bonds. The sponges underwent a complex preparation procedure before the XPS analysis; therefore, their XPS spectrum differs from the ideal XPS spectrum of peptide. It is later treated as a fingerprint for the real biological material.

The XPS C 1s spectrum of the lipase immobilized on the spongin has a maximum at a binding energy of 285.3 eV, and its width is relatively large. The envelope of this spectrum is not identical but relatively close to the envelope observed for lipase. Microscopic analysis of this sample indicates that lipase agglomerates are attached to the fibrous structure of the spongin. This means that part of the surface is covered with lipase, but there is still a part of the spongin fiber free of the enzyme. This composition gives a superposition of the XPS signals coming from lipase and the uncovered spongin, and explains the shift of the C 1s peak maximum. Analysis of the C 1s line provides direct confirmation of lipase immobilization.

The XPS N 1s spectrum acquired from the obtained biocatalytic system is not identical to the XPS N 1s line observed for pure lipase powder (see Figure 5). The maximum of this spectrum is located at 400.2 eV. The envelope of the product is similar to the envelope observed for spongin-based scaffolds, while the N 1s line from lipase has a maximum at 399.7 eV. The C 1s spectrum is regarded as the most representative for the general chemical composition of the surface of the samples considered. It indicates that most of the surface is covered by lipase molecules. Moreover, the lipase structure contains many more nitrogen atoms than was observed for the surface of the spongin. Hence, most of the nitrogen atoms that contribute to the N 1s signal are expected to come from the lipase structure. Therefore the similarity between the envelopes of N 1s lines from spongin and the system after lipase immobilization is considered to be coincidental. However, the shift between the N 1s lines from free

and immobilized lipase is considered to reflect the slight changes of chemical bonding in lipase induced by immobilization on the spongin surface.

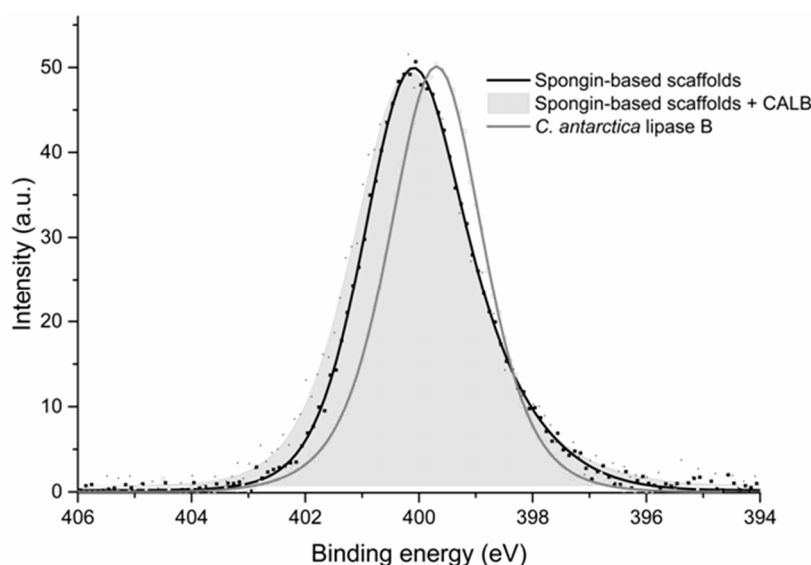


Figure 5. X-ray photoelectron spectroscopy (XPS) N 1s spectra for *C. antarctica* lipase B, spongin-based scaffolds and the product after immobilization of lipase.

Lipase is a macromolecule combining about 350 amino acids [40]. Therefore, its XPS spectrum is an average of multiple binding environments. Considering the N 1s line, the contribution from peptide bonds present in the lipase structure is expected to be the most prominent. The location of the N 1s line maximum for peptide bonds is usually reported to lie between 399.4 and 399.8 eV for proteins and more complicated peptides [41,42] while for simple peptides a value of about 400.1 eV is given [43]. The binding energy observed for pure lipase in the present experiments (399.7 eV) corresponds well with the former range. After immobilization, a shift of about 0.5 eV is observed for the N 1s line.

Considering the results obtained from other experimental techniques used in this study, the formation of hydrogen bonds between lipase and spongin is suggested. Unfortunately, because of the lack of direct XPS detection of hydrogen, the reasoning considering hydrogen bonding is limited. Attempts were made to explain the effects of hydrogen bond formation on the N 1s spectrum in a chemical environment similar to one considered by Kerber et al. [44]. In a complex system where $-N-H-N-$ or $-N-H-O-$ bonds are formed, the XPS patterns feature a positive shift in the N 1s line, as is observed in the present study. The magnitude of the shift can be as much as 1 eV. However, in the case of the macromolecule of lipase, only some of the peptide bonds are expected to participate in bonding with the surface of the spongin fibers. Therefore, the average effect on the N 1s line shift is smaller. This effect seems to be indirect evidence of the formation of hydrogen bonds during the immobilization of lipase on spongin-based scaffolds.

2.5. A Proposed Mechanism for CALB Attachment

It is important to evaluate the effect of the interactions on the properties of the resulting enzyme—spongin systems. For this purpose, this work attempted to determine the mechanism of the enzyme particles attachment. Based on the results obtained (FTIR, ^{13}C NMR and XPS) it is claimed that the mechanism is based on the formation of hydrogen bonds, as presented in Figure 6.

Numerous carboxyl, hydroxyl as well as amine groups, characteristic for the specific amino acids that build spongin fibers, are present in the structure of the marine sponges skeletons [45]. Moreover, the presence of $-NH_2$ groups in the enzyme particles allows the creation of stable hydrogen interactions between the immobilized lipase and the surface of the spongin [46]. Subtle changes in the intensity

and position of certain peaks in the FTIR and ^{13}C CP MAS NMR spectra of the samples before and after immobilization also suggest the formation of hydrogen bonds. However, creation of the limited number of ionic interactions, acid-basic forces, as well as chemical bonds cannot be excluded, as it was mentioned by Macario et al. [47].

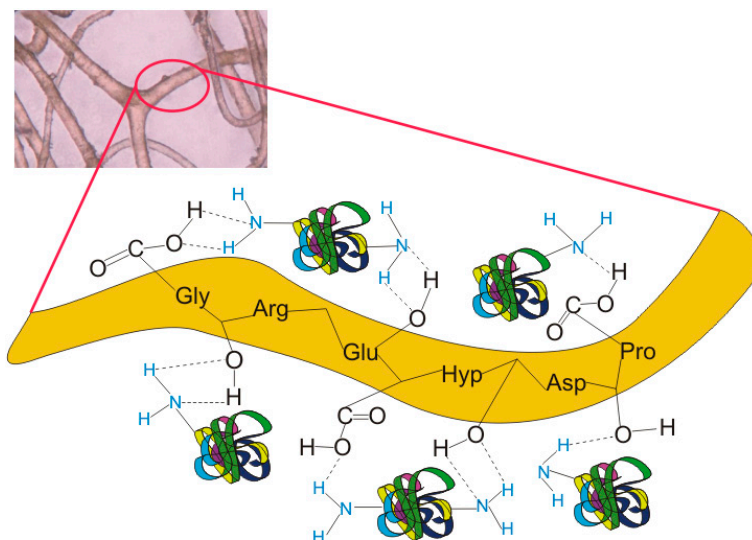


Figure 6. Mechanism of the attachment of lipase B from *C. antarctica* to the surface of spongin fiber.

It should be emphasized that attachment of the enzyme to the spongin surface via hydrogen bonds helps to retain the high catalytic properties of the immobilized lipase. Similar observations were made by Zhang et al. [48]. They assumed that retention of biocatalytic activity might be explained by the fact that interference of the matrix functional groups in the structure of the peptide is limited, thus no significant changes occur.

2.6. Lipase Activity Recovery

The activity of lipase immobilized on spongin-based scaffolds was optimized by adjustment of several reaction parameters. The results, obtained for the systems following immobilization characterized by the highest catalytic activity retention, are presented in Figure 7. They clearly show that its value strongly depends on all parameters of the immobilization process.

The best catalytic properties were found when immobilization was carried out at a temperature of 4 °C, irrespective of process duration and initial enzyme concentration. This is the optimum temperature for storage of the protein, thus the stability of the enzyme structure is maintained. Immobilization carried out at 20 and 50 °C resulted in a slight decrease in catalytic activity recovery, possibly caused by partial inactivation of the biocatalyst during immobilization.

The catalytic properties increase continuously with prolongation of the immobilization time for both initial enzyme solutions and reached maximum after 60 min of the process duration. After that process time relative activity of the produced biocatalytic systems decrease. This finding is consistent with the results of past studies by Zhang et al. [49], which suggest that overloading of the enzyme particles creates steric hindrance effects and diffusional limitations. Moreover, adsorption of the lipase from this solution (concentration 3 mg/mL) produces systems with higher relative activity (up to 20%) in comparison with products following immobilization in the same conditions from an initial solution at a concentration of 1 mg/mL.

The highest relative activity (89%) is observed after 60 min of immobilization at 4 °C from a 3 mg/mL enzyme solution. Therefore, this biocatalytic system was selected for further analysis to determine its stability and reusability.

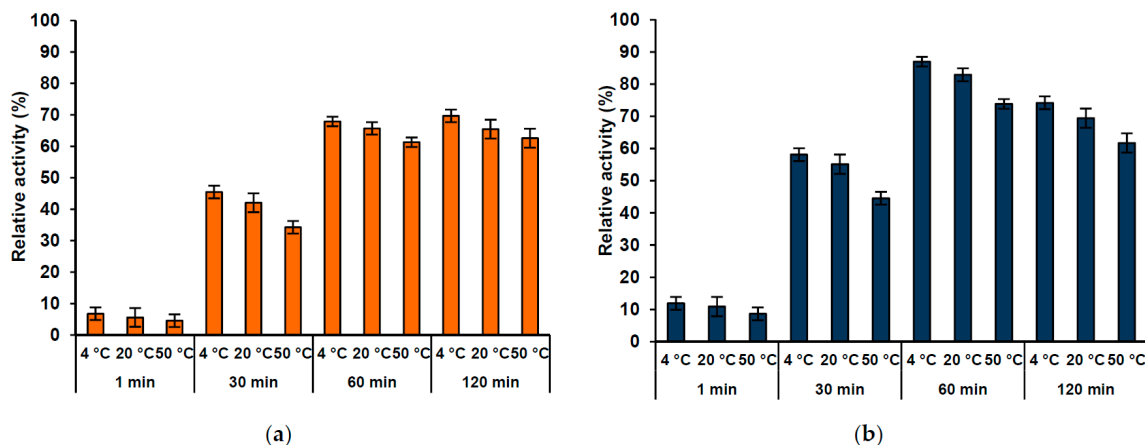


Figure 7. Immobilized lipase activity recovery as a function of temperature and process duration. The process was carried out at pH 7 from lipase solution at concentrations of: 1 mg/mL (a); and 3 mg/mL (b).

2.7. Immobilized Lipase Stability

The effect of temperature and pH on the activity of immobilized CALB was measured based on a hydrolysis reaction over the temperature range 10–80 °C, at pH 7 and in the pH range 3–11 at 40 °C. The results are presented in Figure 8.

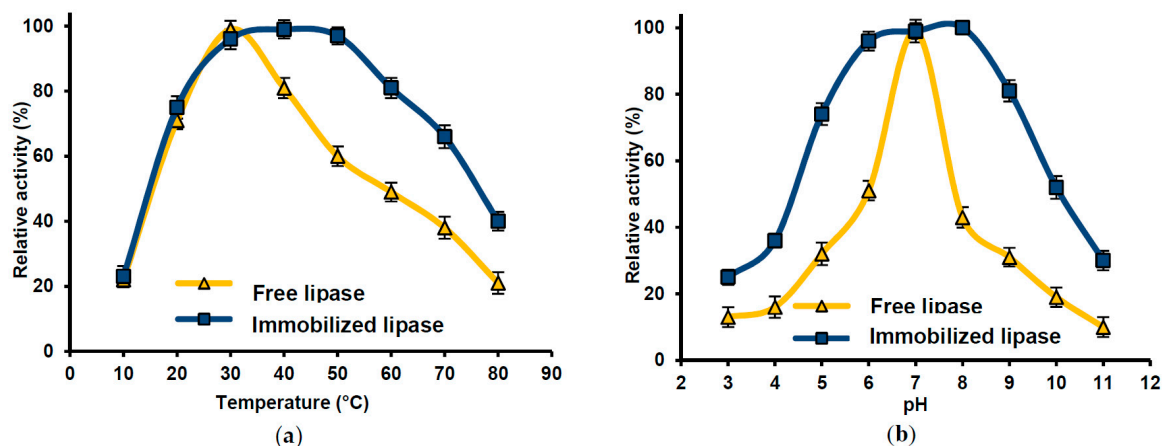


Figure 8. Effect of: temperature (a); and pH (b) on the catalytic activity of free and immobilized lipase B from *C. antarctica* (immobilization conditions: pH 7, $T = 4$ °C, $t = 60$ min, $C_{enz} = 3$ mg/mL).

The optimum temperatures for free and immobilized lipase are 30 and 40 °C respectively. The free enzyme preserved over 80% of its initial activity at 30 and 40 °C, while the immobilized peptide did so over a broader temperature range, from 30 to 60 °C. Lipase B from *C. antarctica* exhibits maximum activity at pH 7, whilst for the immobilized enzyme the equivalent value is pH 8. Lipase attached to the marine sponge retains over 90% of its initial activity in the pH range 6–9, whereas even slight changes in the reaction environment cause a decrease in the hydrolytic properties of the free lipase.

Improvement of thermal and chemical stability is an effect of the interactions created between the enzyme and the support. These protect the tertiary and quaternary structure of the enzyme from conformational changes. Additionally, binding of the enzyme to the carrier stabilizes the whole enzyme particle and preserves it against denaturation under harsh reaction conditions [50]. The results presented by Zhu et al. [51] also show an increase in the pH resistance of the immobilized lipase.

Cabrera-Padilla et al. reported that lipase from *Candida rugosa* immobilized on poly (3-hydroxybutyrate-co-hydroxyvalerate) in the pH up to 6.5 exhibit less than 40% of its relative activity [52]. In contrast, Elnashar et al. immobilized lipase onto grafted alginate-carrageenan beads via covalent bonding. They have found that immobilized lipase shows over 80% of its activity in narrower temperature range (45–55 °C) than lipase immobilized onto *H. communis* spongin-based scaffold [53]. Thus, use of the spongin-based biopolymer makes it possible to obtain even more stable biocatalytic system over a wider pH range, than previously published data.

For the potential application of the biocatalyst systems in industrial processes, it is very important to determine immobilized lipase storage and operational stability. The effect of the storage time and temperature and the number of repeated cycles on the activity of the immobilized enzyme is presented in Figure 9.

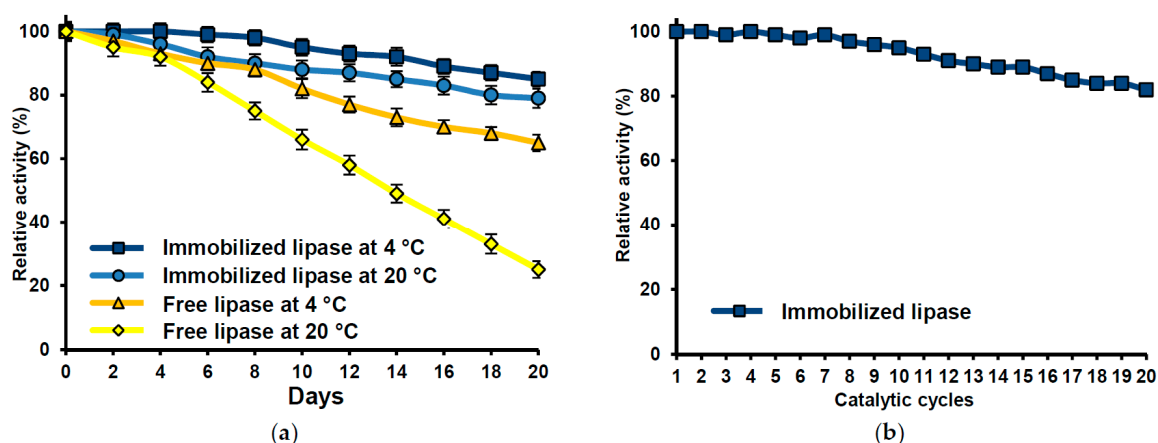


Figure 9. Effect of storage time at various temperatures (a); and repeated reaction cycles (b) on the catalytic activity of free and immobilized lipase B from *C. antarctica* (immobilization conditions: pH 7, $T = 4\text{ }^{\circ}\text{C}$, $t = 60\text{ min}$, $C_{enz} = 3\text{ mg/mL}$).

Immobilized lipase exhibits good reusability, while free lipase, due to its solubility, cannot be reused and recycled for successive reaction cycles. The creation of relatively strong interactions between the enzyme and support stabilizes the peptide particles. Additionally, stable interactions restrict leaching of the enzyme from the matrix [54]. Thereby, immobilized lipase possesses good reusability even after 20 catalytic cycles (over 80% of the initial activity). These results are in good accordance with the data presented by Bencze et al., demonstrating that immobilized *C. antarctica* lipase B retains about 90% of its initial activity [55]. However, Gremos et al. presented that commercial lipase B from *Candida antarctica* immobilized onto acrylic resin, after three catalytic cycles exhibit less than 70% of its initial activity [56]. This proved that CALB attached to the biopolymer matrix possesses much better reusability than lipase attached to the polymeric resins. Moreover, reusability of the attached enzyme is facilitated by the easy separation of the obtained systems by simple centrifugation.

Free lipase is unstable in buffer solution and its activity rapidly decreases, especially when stored at 20 °C (see Figure 9a). After 20 days of storage under these conditions the free enzyme retains less than 30% of its initial activity. Immobilization of *C. antarctica* lipase B improves the hydrolytic properties of the enzyme. Irrespective of storage temperature, after the same time, the biocatalysts attached to the sponge matrix retain over 80% of their initial activity. This phenomenon can be explained by the fact that the spongin-based scaffold protects the enzyme particles against inactivation by components of the reaction mixture [34]. CALB immobilized onto *H. communis* spongin-based scaffolds after storage for 20 days at 4 °C retain over 90% of its initial activity. In comparison, lipase from *Candida rugosa* immobilized on sporopollenin from *Lycopodium clavatum* after storage in the same conditions exhibit less than 75% of its initial activity [57]. These results suggest that used in this study biopolymer helps to hold good catalytic properties of the immobilized lipase for a longer period of time.

2.8. Kinetic Parameters

C. antarctica lipase B immobilized on spongin-based scaffolds was analyzed for changes in kinetic parameters in comparison with the free enzyme. The Michaelis–Menten constant (K_m) and V_{max} were from a Lineweaver–Burk plot with various initial *p*-NPP concentrations under optimal reaction conditions.

The K_m value of the free enzyme was 5.26 ± 0.47 mM, while for immobilized lipase the value is slightly higher, at 6.03 ± 0.52 mM. This suggests that sponge-bonded lipase has slightly lower affinity toward its substrates. Small changes in the K_m value for immobilized lipase were also noted by Talbert et al. [58]. The lower value of V_{max} for the immobilized enzyme (15.62 ± 0.94 U/mg) in comparison with free lipase (17.45 ± 0.97 U/mg) confirms the previous observations. These findings could be explained by steric effects that lead to blocking of enzymatic active sites after immobilization. Moreover, some conformational changes in the enzyme structure may occur during immobilization and may provide an additional explanation of the decrease in catalytic activity [59]. Obtained results stay in agreement with the results for catalytic activity retention (see Figure 7b).

In contrast, when lipase from *Candida antarctica* was immobilized onto silica SBA-15 almost five-times higher value of the Michaelis–Menten constant and five-times lower value of the V_{max} were noticed [60]. Thus, presented in this work results suggest that open network of the used spongin-based scaffolds reduce diffusional limitation and facilitate maintaining of the high catalytic properties by immobilized CALB.

2.9. Rapeseed Oil Transesterification

The biocatalytic systems with CALB immobilized on spongin-based scaffolds were used in processes of transesterification of rapeseed oil. Results of the methanolysis of the oil over different reaction conditions are given in Table 3 and Figure 10.

The most important factors influencing the conversion ratio were the process temperature and pH. Total conversion of oil samples was observed at 40 °C and pH 10, when the oil-to-methanol molar ratio was 1:13.3 and the reaction lasted for 24 h (sample 14). Changing the oil-to-methanol molar ratio to 1:5.3 caused the conversion to fall to 64.9% (sample 16). The differences between the samples with pH 7 were significant, and the conversion did not exceed 3.1%.

Table 3. Influence of the process parameters on conversion of rapeseed oil triglycerides into fatty acids methyl esters (FAME) and glycerol using the immobilized lipase, where n_o/n_m denotes the molar ratio of oil to methanol.

Sample Number	Temperature (°C)	pH	n_o/n_m	Time (h)	Conversion (%)	TG (% w/w)	FAME (% w/w)	Glycerol (% w/w)
1	20	7	1:13.3	1	0.9 ± 0.1	99.1 ± 0.1	0.8 ± 0.1	0.1 ± 0.1
2				0.6 ± 0.1	99.4 ± 0.1	0.6 ± 0.1	0.0 ± 0.1	
3			1:5.3	1	0.7 ± 0.1	99.3 ± 0.1	0.7 ± 0.1	0.0 ± 0.1
4				0.4 ± 0.1	99.6 ± 0.1	0.4 ± 0.1	0.0 ± 0.1	
5		10	1:13.3	1	18.5 ± 0.5	81.5 ± 0.5	16.9 ± 0.5	1.6 ± 0.1
6				31.1 ± 0.7	68.9 ± 0.7	28.4 ± 0.7	2.7 ± 0.2	
7			1:5.3	1	13.4 ± 0.4	66.7 ± 0.7	31.1 ± 0.7	2.2 ± 0.1
8				33.3 ± 0.7	86.6 ± 0.4	12.5 ± 0.7	0.9 ± 0.1	
9	40	7	1:13.3	1	1.4 ± 0.1	98.6 ± 0.1	1.3 ± 0.1	0.1 ± 0.1
10				3.1 ± 0.2	96.9 ± 0.2	2.8 ± 0.21	0.3 ± 0.1	
11			1:5.3	1	0.4 ± 0.1	99.6 ± 0.1	0.4 ± 0.1	0.0 ± 0.1
12				0.8 ± 0.1	99.2 ± 0.1	0.8 ± 0.1	0.0 ± 0.1	
13		10	1:13.3	1	21.1 ± 0.4	78.9 ± 0.4	19.3 ± 0.4	1.8 ± 0.2
14				99.1 ± 0.9	0.0 ± 0.9	91.4 ± 0.9	8.6 ± 0.5	
15			1:5.3	1	27.5 ± 0.6	72.5 ± 0.6	25.7 ± 0.6	1.8 ± 0.2
16				64.9 ± 0.8	35.1 ± 0.8	60.7 ± 0.8	4.2 ± 0.3	

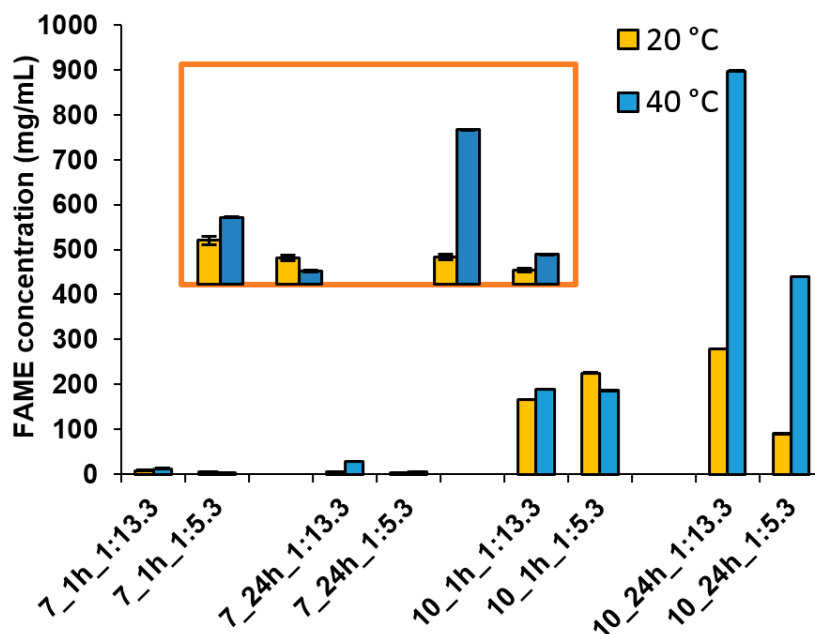


Figure 10. Effect of the various reaction parameters on fatty acids methyl esters (FAME) concentration after conversion of rapeseed oil using immobilized lipase.

A study by Verdugo et al. [29] conducted with ethanol indicated 20 °C as the optimum temperature. However, in that study a non-immobilized enzyme was used. A study by Calero et al. [61] using immobilized lipase showed that the highest conversion occurs at 40 °C. These results correspond with those obtained in the present study. The fact that the best conversion occurs at that temperature may be related to the fact that the maximum activity of immobilized lipase is also observed at 40 °C (see Figure 8a).

The values of conversion ratio correspond to measurements of FAME concentration in the samples. Its highest content, almost 900 mg/mL, was observed in the sample with total conversion (sample 14). A drop in temperature from 40 to 20 °C results in a reduction of FAME concentration to 280 mg/mL. When the hydrolysis time was 1 h, the influence of temperature on the final quantity of FAME amount was practically negligible. Dizge and Keskinler [62] also obtained the best results for transesterification of canola oil into FAME and glycerol at 40 °C using immobilized lipase as catalyst; however, they applied a relatively high (6:1) methanol–oil molar ratio.

The biggest advantage of the *H. communis* spongin-based scaffold is its open, three-dimensional fibrous network that enables easy contact of the substrates with the active sites of the lipases, thus reducing the diffusional limitations. Moreover, porosity of the marine sponge scaffolds and the presence of many hydrophilic groups on its surface caused that glycerol might be adsorbed more often in these places, than onto the enzyme particles, that protect lipase before clogging, as it was reported earlier by Xu et al. [63].

The experiments proved that the lipase immobilized on 3D spongin-based scaffolds is an efficient catalyst of the transesterification reaction, allowing a high FAME concentration to be obtained after the process. Moreover, the conversion of rapeseed oil using the immobilized enzyme may be a promising source of glycerol, a substrate of interest to many branches of industry.

3. Materials and Methods

3.1. Materials

Hippospongia communis sponges, collected on the Mediterranean coast in Tunisia, were purchased from INTIB GmbH (Freiberg, Germany). Acetic acid, sodium acetate, sodium phosphate monobasic,

sodium phosphate dibasic and tris(hydroxymethyl) aminomethane were supplied by Sigma-Aldrich (St. Louis, MO, USA). Sodium hydroxide, methanol, ethanol, propan-2-ol, orthophosphoric acid and hydrochloric acid (all laboratory grade) were purchased from Chempur (Gliwice, Poland). Lipase type B from *Candida antarctica* (CALB) (isoelectric point in the range 6.0–6.5), Coomassie Brilliant Blue G-250, *para*-nitrophenyl palmitate (*p*-NPP), *para*-nitrophenol (*p*-NP), gum arabic and Triton X-100 (laboratory grade) were supplied by Sigma-Aldrich (St. Louis, MO, USA). Commercially available rapeseed oil, used in the transesterification reaction, was provided by a local company (ADM Company, Szamotuły, Poland).

3.2. Preparation of Spongin-Based Scaffolds from *Hippospongia communis* Demosponge

For the proper preparation of the spongin-based scaffolds from *H. communis* demosponges their cell- and debris-free skeletons were initially washed with distilled water to dissolve water soluble salts. After that selected skeletons were immersed in 3 M HCl for 72 h at 24 °C to dissolve possible calcium carbonate microparticles of natural origin. The scaffolds (Figure 11) were rinsed with distilled water until the pH reached 7. Finally, the spongin-based scaffolds were dried at 50 °C for 24 h and stored in plastic bags at room temperature.



Figure 11. Purified 3D spongin-based scaffold isolated from *H. communis* demosponge.

3.3. Lipase Immobilization

An amount of 500 mg of the previously prepared spongin scaffolds were placed in a reactor, and 10 mL of CALB solution at a concentration of 1 or 3 mg/mL was added. The mixture was then placed on a shaker (IKA Werke GmbH, Staufen im Breisgau, Germany) for a specified period of time (from 1, 30, 60 and 120 min). After the process, obtained biocatalytic systems were centrifuged for 20 min (4000 rpm at the temperature of 4 °C) and dried for 48 h at ambient temperature.

3.4. Analysis of Products Following Immobilization

SEM images were recorded on an EVO40 scanning electron microscope (Zeiss, Munich, Germany). Samples were first coated with Au for a 15 s by PV205P coater (Balzers, Zurich, Switzerland).

Digital images of the spongin scaffolds and the products following immobilization were created using a VHX 5000 digital microscope (Keyence, Osaka, Japan).

FTIR spectra of the spongin-scaffolds, free lipase and the product following the immobilization were made using Vertex 70 (Bruker Optics, Billerica, MA, USA) apparatus. Substances were analyzed as KBr pellets (wavenumber range of 4000–400 cm^{-1} , resolution of 0.5 cm^{-1}).

^{13}C CP MAS NMR spectra were obtained on a Bruker DSX spectrometer (Bruker Optics, Billerica, MA, USA). Before measurement around 100 mg of the sample was selected samples of approximately 100 mg were placed in a ZrO_2 rotator at a diameter of 4 mm. Measurements were made using single pulse excitation with high-power proton decoupling at 100.63 MHz in a standard MAS probe (spinning speed of 8 kHz, pulse repetition 10 s).

X-ray photoelectron spectroscopy (XPS) was performed using Al K α ($h\nu = 1486.6$ eV) radiation in a Prevac system (Prevac, Rogów, Poland). The electron energy analyzer Scienta SES 2002 (Scienta Omicron, Taunusstein, Germany) operated at constant transmission energy ($E_p = 50$ eV). The spectrometer was calibrated according to the photoemission lines of energy bonding (EB): EB Cu $2p_{3/2} = 932.8$ eV, EB Ag $3d_{5/2} = 368.3$ eV and EB Au $4f_{7/2} = 84.0$ eV.

The carbon conductive double-sided adhesive discs were used to attach the samples to a molybdenum sample holder. Correction of charging effects was done assuming that the C 1s line component corresponding to aliphatic carbon bindings (CH_x) is located at the binding energy of 284.8 eV.

3.5. Hydrolytic Activity

The relative hydrolytic activity was estimated based on the spectrophotometric measurements during model reaction of *para*-nitrophenyl palmitate hydrolysis, using previously published procedure with slight modifications [64]. The amount of the released *p*-NP was measured at $\lambda = 410$ nm by using Jasco V-750 UV-Vis spectrophotometer (Jasco, Tokyo, Japan). The relative activities of the immobilized CALB were calculated using a standard calibration curve for *p*-NP. The amount of biocatalyst that liberates 1 μ mol *p*-NP per minute is defined as the one unit of lipase activity. All reactions, made in triplicate, were conducted for 2 min at 30 °C with stirring at 1000 rpm. In the hydrolysis process 10 mg of the free lipase and an appropriate amount of the product following immobilization containing 10 mg of the enzyme was used. Amount of the immobilized lipase was evaluated according to Bradford method [65]. The retention of the catalytic activity (A_R) of the immobilized lipase was calculated according to following equation:

$$A_R = \frac{A_I}{A_0} \times 100\%$$

where: A_0 denotes the total initial activity of the free enzyme, and A_I denotes the activity of the immobilized lipase.

3.6. Stability of Immobilized Lipase

To evaluate effect of pH, temperature, storage time and number of catalytic cycles on the relative activity of the free and immobilized lipase, hydrolysis reaction of *p*-NPP into *p*-NP was used. All measurements were made in triplicate. The relative activities of the immobilized CALB were calculated using standard calibration curve of *p*-NP.

Effect of pH on the activity of the immobilized protein was evaluated in the pH range 3–11. Activity of the analyzed systems was measured spectrophotometrically after their incubation in a buffer solution at the appropriate pH for 2 h.

Effect of temperature on the products following immobilization was estimated in a temperature range from 10 to 80 °C. For this purpose, hydrolysis reaction was carried out at the desired temperature.

The relative activity was evaluated every 2 days for free and immobilized form of lipase stored for 20 days in a buffer at pH 7, at both 4 and 20 °C.

Activity retention of the immobilized lipase during repeated recovery cycles was evaluated over 20 catalytic cycles. Immobilized lipase was centrifuged from the reaction mixture after each reaction cycle, washed with 10 mL of phosphate buffer, dried, and used to catalyze the next reaction cycle.

3.7. Kinetic Parameters

The Michaelis–Menten constant (K_m) and the maximum rate of reaction (V_{max}) of the free and immobilized lipase were evaluated based on the hydrolysis of *p*-NPP under optimal reaction conditions with various concentrations of *p*-NPP. According to Lineweaver–Burk plots apparent kinetic parameters (K_m and V_{max}) were calculated.

3.8. Rapeseed Oil Transesterification

To evaluate the effectiveness of rapeseed oil bioconversion the transesterification experiments were conducted as follows. To 100 mL glass flasks, 5 mg of the immobilized lipase, and 10 mL of rapeseed oil and methanol (molar ratio 1:5.3 or 1:13.3) were added. When necessary, in order to maintain the pH 10, few microliters of 0.1 M NaOH solution was added to the samples. Then, the samples were incubated on a shaker platform in different incubation time (1 or 24 h), temperature (20 or 40 °C) and pH (7 or 10). In all experiments the immobilized lipase retaining the highest catalytic activity was used. The most convenient conditions of the immobilization process (2 h process duration, 4 °C, pH 7) were established at previous stages of the study.

FAME and glycerol quantification analysis based on the method described by Luna et al. [28]. A gas chromatograph coupled with mass spectrometer (Pegasus 4D GCxGC-TOFMS, LECO Corp., St. Joseph, MO, USA) with a capillary column (BPX5—5% phenyl equivalent, SGE Int., Melbourne, Australia) was used. The ion source and transfer line temperature were set at 250 °C. As the carrier gas helium was applied (a flow rate of 1.0 mL/min). One microliter of the sample was injected in split mode (1:99). The oven temperature was set and at 55 °C maintained for 5 min, then a heating ramp was applied up to 300 °C at a rate of 10 °C/min, and the temperature of the oven was maintained at 300 °C for 15 min. As an internal standard, hexadecane was used. The transesterification efficiency of the immobilized lipase was presented as the conversion ratio, which is defined as the ratio of the mass of produced FAME to the theoretical mass of FAME after total transesterification.

4. Conclusions

In this work, spongin-based scaffolds were used for the first time as a support for the immobilization of lipase B from *C. antarctica*. Highly sensitive methods such as XPS and ¹³C CP MAS NMR were used not only to prove the immobilization of the lipase, but also to determine the mechanism by which this enzyme is attached to the spongin surface, which is most probably based on hydrogen bonds. Analysis showed that the highest catalytic activity is maintained after a process carried out for 60 min at a temperature of 4 °C and pH 7. Moreover, immobilized lipase exhibits a significant improvement in thermal and chemical stability in comparison with free lipase, and retains over 80% of its initial activity even after 20 days of storage at 4 °C or after catalyzing 20 reaction cycles. The biocatalytic systems were used as catalysts in the transesterification reaction of rapeseed oil with methanol. The results clearly show that lipase immobilized on marine sponge, under optimal conditions, enables 100% conversion of the triglycerides to FAME and glycerol. This work presents a useful protocol to produce stable and active immobilized CALB on the surface of spongin-based scaffolds, which may also be applied to immobilization of other enzymes.

Acknowledgments: The work was supported by National Science Centre Poland Research Grant no. DEC-2015/19/N/ST8/02220 as well as by the DFG Grant HE/394-3 (Germany).

Author Contributions: Jakub Zdarta planned studies, evaluated enzyme immobilization efficiency, immobilized enzyme activity and stability, and developed results. Małgorzata Norman prepared functional biosorbent and carried out the immobilization experiments. Wojciech Smułek carried out the transesterification reactions and developed the results of the GC-MS analysis. Dariusz Moszyński developed the results of the XPS analysis. Ewa Kaczorek supervised the manuscript preparation and interpreted the data. Allison L. Stelling supervised the manuscript preparation and interpreted the data. Hermann Ehrlich planned studies and developed results. Teofil Jesionowski coordinated of all tasks in the paper, planned studies, developed the results and participated in discussions.

Conflicts of Interest: The authors declare no conflicts of interest.

References

1. Rosevear, A. Immobilised biocatalysts—A critical review. *J. Chem. Technol. Biotechnol.* **1984**, *34*, 127–150. [[CrossRef](#)]

2. Jesionowski, T.; Zdarta, J.; Krajewska, B. Enzyme immobilization by adsorption: A review. *Adsorption* **2014**, *20*, 801–821. [[CrossRef](#)]
3. Guzik, U.; Hupert-Kocurek, K.; Wojcieszńska, D. Immobilization as a strategy for improving enzyme properties-application to oxidoreductases. *Molecules* **2014**, *19*, 8995–9018. [[CrossRef](#)] [[PubMed](#)]
4. Matosevic, S.; Szita, N.; Baganz, F. Fundamentals and applications of immobilized microfluidic enzymatic reactors. *J. Chem. Technol. Biotechnol.* **2011**, *86*, 325–334. [[CrossRef](#)]
5. Nicolini, J.V.; de Resende, N.S.; Ferraz, H.C. Adsorption of horseradish peroxidase onto titanate nanowires. *J. Chem. Technol. Biotechnol.* **2015**, *90*, 739–746. [[CrossRef](#)]
6. Wang, F.; Guo, C.; Liu, H.-Z.; Liu, C.-Z. Immobilization of *Pycnoporus sanguineus* laccase by metal affinity adsorption on magnetic chelator particles. *J. Chem. Technol. Biotechnol.* **2008**, *83*, 97–104. [[CrossRef](#)]
7. Yewle, J.N.; Wei, Y.; Puleo, D.A.; Daunert, S.; Bachas, L.G. Oriented immobilization of proteins on hydroxyapatite surface using bifunctional bisphosphonates as linkers. *Biomacromolecules* **2012**, *13*, 1742–1749. [[CrossRef](#)] [[PubMed](#)]
8. Banjanac, K.; Mihailović, M.; Prlainović, N.; Stojanović, M.; Carević, M.; Marinković, A.; Bezbradica, D. Cyanuric chloride functionalized silica nanoparticles for covalent immobilization of lipase. *J. Chem. Technol. Biotechnol.* **2016**, *91*, 439–448. [[CrossRef](#)]
9. Tavares, A.P.M.; Silva, C.G.; Drazic, G.; Silva, A.M.T.; Loureiro, J.M.; Faria, J.L. Laccase immobilization over multi-walled carbon nanotubes: Kinetic, thermodynamic and stability studies. *J. Colloid Interface Sci.* **2015**, *454*, 52–60. [[CrossRef](#)] [[PubMed](#)]
10. Mohamad, N.R.; Marzuki, N.H.C.; Buang, N.A.; Huyop, F.; Wahab, R.A. An overview of technologies for immobilization of enzymes and surface analysis techniques for immobilized enzymes. *Biotechnol. Biotechnol. Equip.* **2015**, *29*, 205–220. [[CrossRef](#)] [[PubMed](#)]
11. Datta, S.; Christena, L.R.; Rajaram, Y.R.S. Enzyme immobilization: An overview on techniques and support materials. *3 Biotech* **2013**, *3*, 1–9. [[CrossRef](#)] [[PubMed](#)]
12. Krajewska, B. Application of chitin- and chitosan-based materials for enzyme immobilizations: A review. *Enzym. Microb. Technol.* **2004**, *35*, 126–139. [[CrossRef](#)]
13. Saeed, A.; Iqbal, M. Loofa (*Luffa cylindrica*) sponge: Review of development of the biomatrix as a tool for biotechnological applications. *Biotechnol. Prog.* **2013**, *29*, 573–600. [[CrossRef](#)] [[PubMed](#)]
14. Pallela, R.; Ehrlich, H. *Marine Sponges: Chemicobiological and Biomedical Applications*; Springer International Publishing AG: New York, NY, USA, 2016.
15. Dahlmans, J.J.; Meijerink, T.A.J. Insoluble Carrier-Bound Enzymes. U.S. Patent 3,919,048, 11 November 1975.
16. Chen, J.P.; Lin, T.C. Loofa sponge as a scaffold for culture of Rat hepatocytes. *Biotechnol. Prog.* **2008**, *21*, 315–319. [[CrossRef](#)] [[PubMed](#)]
17. Annunciado, T.R.; Sydenstricker, T.H.D.; Amico, S.C. Experimental investigation of various vegetable fibers as sorbent materials for oil spills. *Mar. Pollut. Bull.* **2005**, *50*, 1340–1346. [[CrossRef](#)] [[PubMed](#)]
18. Ehrlich, H.; Maldonado, M.; Hanke, T.; Meissner, H.; Born, R. Spongins: Nanostructural investigations and development of biomimetic material model. *VDI Berichte* **2003**, *1803*, 287–292.
19. Kim, M.M.; Mendis, E.; Rajapakse, N.; Lee, S.H.; Kim, S.K. Effect of spongin derived from *Hymeniacidon sinapium* on bone mineralization. *J. Biomed. Mater. Res. Part B* **2009**, *90B*, 540–546. [[CrossRef](#)] [[PubMed](#)]
20. Green, D.W.; Howard, D.; Yang, X.; Kelly, M.; Oreffo, R.O. Natural marine sponge fiber skeleton: A biomimetic scaffold for human osteoprogenitor cell attachment, growth, and differentiation. *Tissue Eng.* **2003**, *9*, 1159–1166. [[CrossRef](#)] [[PubMed](#)]
21. Green, D.W. Tissue bionics: Examples in biomimetic tissue engineering. *Biomed. Mater.* **2008**, *3*, 034010. [[CrossRef](#)] [[PubMed](#)]
22. Green, D.W.; Padula, M.P.; Santos, J.; Chou, J.; Milthorpe, B.; Ben-Nissan, B. A therapeutic potential for marine skeletal proteins in bone regeneration. *Mar. Drugs* **2013**, *11*, 1203–1220. [[CrossRef](#)] [[PubMed](#)]
23. Norman, M.; Bartczak, P.; Zdarta, J.; Tylus, W.; Szatkowski, T.; Stelling, A.L.; Ehrlich, H.; Jesionowski, T. Adsorption of C.I. Natural Red 4 onto spongin skeleton of marine demosponge. *Materials* **2015**, *8*, 96–116. [[CrossRef](#)]
24. Derewenda, Z.S.; Derewenda, U.; Dodson, G.G. The crystal and molecular structure of the *Rhizomucor miehei* triacylglyceride lipase at 1.9 Å resolution. *J. Mol. Biol.* **1992**, *227*, 818–839. [[CrossRef](#)]

25. Palomo, J.M.; Munoz, G.; Fernandez-Lorente, G.; Mateo, C.; Fernandez-Lafuente, R.; Guisan, J.M. Interfacial adsorption of lipases on very hydrophobic support (octadecyl-Sepabeads): Immobilization, hyperactivation and stabilization of the open form of lipases. *J. Mol. Catal. B* **2008**, *19*, 279–286. [[CrossRef](#)]
26. Silva, N.C.A.; Mirandaa, J.S.; Bolina, I.C.A.; Silva, W.C.; Hiratac, D.B.; de Castro, H.F.; Mendes, A.A. Immobilization of porcine pancreatic lipase on poly-hydroxybutyrate particles for the production of ethyl esters from macaw palm oils and pineapple flavor. *Biochem. Eng. J.* **2014**, *82*, 139–149. [[CrossRef](#)]
27. Hernández, K.; Garcia-Galan, C.; Fernández-Lafuente, R. Simple and efficient immobilization of lipase B from *Candida antarctica* on porous styrene–divinylbenzene beads. *Enzym. Microb. Technol.* **2011**, *49*, 72–78. [[CrossRef](#)] [[PubMed](#)]
28. Mendes, A.A.; Rodrigues, D.S.; Filice, M.; Fernández-Lafuente, R.; Guisán, J.M.; Palomo, J.M. Regioselective monohydrolysis of per-*O*-acetylated-1-substituted- β -glucopyranosides catalyzed by immobilized lipases. *Tetrahedron* **2008**, *64*, 10721–10727. [[CrossRef](#)]
29. Verdugo, C.; Luna, D.; Posadillo, A.; Sancho, E.D.; Rodriguez, S.; Bautista, F.; Luque, R.; Marinas, J.M.; Romero, A.A. Production of a new second generation biodiesel with a low cost lipase derived from *Thermomyces lanuginosus*: Optimization by response surface methodology. *Catal. Today* **2011**, *167*, 107–112. [[CrossRef](#)]
30. Luna, D.; Posadillo, A.; Caballero, V.; Verdugo, C.; Bautista, F.M.; Romero, A.A.; Sancho, E.D.; Luna, C.; Calero, J. New biofuel integrating glycerol into its composition through the use of covalent immobilized pig pancreatic lipase. *Int. J. Mol. Sci.* **2012**, *13*, 10091–10112. [[CrossRef](#)] [[PubMed](#)]
31. Caballero, V.; Bautista, F.M.; Campelo, J.M.; Luna, D.; Marinas, J.M.; Romero, A.A.; Hidalgo, J.M.; Luque, R.; Macario, A.; Giordano, G. Sustainable preparation of a novel glycerol-free biofuel by using pig pancreatic lipase: Partial 1,3-regiospecific alcoholysis of sunflower oil. *Process Biochem.* **2009**, *44*, 334–342. [[CrossRef](#)]
32. Szatkowski, T.; Wysokowski, M.; Lota, G.; Peziak, D.; Bazhenov, V.V.; Nowaczyk, G.; Walter, J.; Molodtsov, S.L.; Stöcker, H.; Himcinski, C.; et al. Novel nanostructured hematite—Spongine composite developed using an extreme biomimetic approach. *RSC Adv.* **2015**, *5*, 79031–79040. [[CrossRef](#)]
33. Norman, M.; Bartzak, P.; Zdarta, J.; Ehrlich, H.; Jesionowski, T. Anthocyanin dye conjugated with *Hippospongia communis* marine demosponge skeleton and its antiradical activity. *Dyes Pigment.* **2016**, *134*, 541–552. [[CrossRef](#)]
34. Zdarta, J.; Jesionowski, T. *Luffa cylindrica* sponges as a thermally and chemically stable support for *Aspergillus niger* lipase. *Biotechnol. Prog.* **2016**, *32*, 657–665. [[CrossRef](#)] [[PubMed](#)]
35. Wong, P.T.T.; Nong, R.K.; Caputo, T.A.; Godwin, T.A.; Rigas, B. Infrared spectroscopy of exfoliated human cervical cells: Evidence of extensive structural changes during carcinogenesis. *Proc. Natl. Acad. Sci. USA* **1991**, *88*, 10988–10992. [[CrossRef](#)] [[PubMed](#)]
36. Portaccio, M.; Della Ventura, B.; Mita, D.G.; Manolova, N.; Stoilova, O.; Rashkov, I.; Lepore, M. FT-IR microscopy characterization of sol–gel layers prior and after glucose oxidase immobilization for biosensing applications. *J. Sol-Gel Sci. Technol.* **2011**, *57*, 204–211. [[CrossRef](#)]
37. Beinert, W.D.; Ruterjans, H.; Muller, F.; Bacher, A. Nuclear magnetic resonance studies of the old yellow enzyme: 2. ^{13}C NMR of the enzyme recombined with ^{13}C -labeled flavin mononucleotides. *Eur. J. Biochem.* **1985**, *152*, 581–587. [[CrossRef](#)] [[PubMed](#)]
38. Zdarta, J.; Klapiszewski, Ł.; Wysokowski, M.; Norman, M.; Kołodziejczak-Radzimska, A.; Moszyński, D.; Ehrlich, H.; Maciejewski, H.; Stelling, A.L.; Jesionowski, T. Chitin-lignin material as a novel matrix for enzyme immobilization. *Mar. Drugs* **2015**, *13*, 2424–2446. [[CrossRef](#)] [[PubMed](#)]
39. Tomizuka, N.; Ota, Y.; Yamada, K. Studies on lipase from *Candida cylindracea*. *Agric. Biol. Chem.* **1966**, *30*, 1090–1096.
40. Uppenberg, J.; Hansen, M.T.; Patkar, S.; Jones, T.A. The sequence, crystal structure determination and refinement of two crystal forms of lipase B from *Candida antarctica*. *Structure* **1994**, *2*, 293–308. [[CrossRef](#)]
41. Rouxhet, P.G.; Genet, M.J. XPS analysis of bio-organic systems. *Surf. Interface Anal.* **2011**, *43*, 1453–1470. [[CrossRef](#)]
42. Porté-Durrieu, M.C.; Labrugere, F.; Villars, F.; Lefebvre, F.; Dutova, S.; Guette, A.; Bordenave, L.; Baquey, C. Development of RGD peptides grafted onto silica surfaces: XPS characterization and human endothelial cell interactions. *J. Biomed. Mater. Res. Part A* **1999**, *46*, 368–375. [[CrossRef](#)]

43. Stevems, J.S.; Luca, M.; Pelendritis, M.; Terenghi, G.; Downes, S.; Schroeder, S.L.M. Quantitative analysis of complex amino acids and RGD peptides by X-ray photoelectron spectroscopy (XPS). *Surf. Interface Anal.* **2013**, *45*, 1238–1246. [[CrossRef](#)]
44. Kerber, S.J.; Bruckner, J.J.; Wozniak, K.; Seal, S.; Hardcastle, S.; Barr, T.L. The nature of hydrogen in X-ray photoelectron spectroscopy: General patterns from hydroxides to hydrogen bonding. *J. Vac. Sci. Technol. A* **1996**, *14*, 1314–1320. [[CrossRef](#)]
45. Garrone, R. The collagen of the Porifera. In *Biology of Invertebrate and Lower Vertebrate Collagens*; Bairati, A., Ed.; Plenum Press: New York, NY, USA, 1985; pp. 157–175.
46. Svendsen, A. Lipase protein engineering. *Biochim. Biophys. Acta* **2000**, *1543*, 223–238. [[CrossRef](#)]
47. Macario, A.; Moliner, M.; Diaz, U.; Jorda, J.L.; Corma, A.; Giordano, G. Biodiesel production by immobilized lipase on zeolites and related materials. *Stud. Surface Sci. Catal.* **2008**, *174*, 1011–1016.
48. Zhang, R.; Xiao, X.; Tai, Q.; Huang, H.; Yang, J.; Hu, Y. Preparation of lignin–silica hybrids and its application in intumescent flame-retardant poly(lactic acid) system. *High Perform. Polym.* **2012**, *24*, 738–745. [[CrossRef](#)]
49. Zhang, D.H.; Zhang, Y.F.; Zhi, G.Y.; Xie, Y.L. Effect of hydrophobic/hydrophilic characteristics of magnetic microspheres on the immobilization of BSA. *Colloids Surfaces B* **2011**, *82*, 302–306. [[CrossRef](#)] [[PubMed](#)]
50. Narwal, S.K.; Saun, N.K.; Gupta, R. Characterization and catalytic properties of free and silica-bound lipase: A comparative study. *J. Oleo Sci.* **2014**, *63*, 599–605. [[CrossRef](#)] [[PubMed](#)]
51. Zhu, Y.T.; Ren, X.Y.; Liu, Y.M.; Wei, Y.; Qing, L.S.; Liao, X. Covalent immobilization of porcine pancreatic lipase on carboxyl-activated magnetic nanoparticles: Characterization and application for enzymatic inhibition assays. *Mater. Sci. Eng.* **2014**, *38*, 278–285. [[CrossRef](#)] [[PubMed](#)]
52. Cabrera-Padilla, R.Y.; Lisboa, M.C.; Fricks, A.T.; Franceschi, E.; Lima, A.S.; Silva, D.P.; Soares, C.M.F. Immobilization of *Candida rugose* lipase on poly (3-hydroxybutyrate-co-hydroxyvalerate): A new eco-friendly support. *J. Ind. Microbiol. Biotechnol.* **2012**, *39*, 289–298. [[CrossRef](#)] [[PubMed](#)]
53. Elnashar, M.M.M.; Mostafa, H.; Morsy, N.A.; Awad, G.E.A. Biocatalysts: Isolation, identification, and immobilization of thermally stable lipase onto three novel biopolymeric supports. *Ind. Eng. Chem. Res.* **2013**, *52*, 14760–14767. [[CrossRef](#)]
54. Dong, L.; Ge, C.; Qin, P.; Chen, Y.; Xu, Q. Immobilization and catalytic properties of *Candida lipolytic* lipase on surface of organic intercalated and modified MgAl-LDHs. *Solid State Sci.* **2014**, *31*, 8–15. [[CrossRef](#)]
55. Bencze, L.C.; Bartha-Vari, B.H.; Katona, G.; Tos, M.I.; Paizs, C.; Irimie, F.D. Nanobioconjugates of *Candida antarctica* lipase B and single-walled carbon nanotubes in biodiesel production. *Bioresour. Technol.* **2016**, *200*, 853–860. [[CrossRef](#)] [[PubMed](#)]
56. Gremos, S.; Kekos, D.; Kolisis, F. Supercritical carbon dioxide biocatalysis as a novel and green methodology for the enzymatic acylation of fibrous cellulose in one step. *Bioresour. Technol.* **2012**, *115*, 96–101. [[CrossRef](#)] [[PubMed](#)]
57. Tutar, H.; Yilmaz, E.; Pehlivan, E.; Yilmaz, M. Immobilization of *Candida rugosa* lipase on sporopollenin from *Lycopodium clavatum*. *Int. J. Biolog. Macromol.* **2009**, *45*, 315–320. [[CrossRef](#)] [[PubMed](#)]
58. Talbert, J.N.; Wang, L.S.; Duncan, B.; Jeong, Y.; Andler, S.M.; Rotello, V.M.; Goddard, J.M. Immobilization and stabilization of lipase (CaLB) through hierarchical interfacial assembly. *Biomacromolecules* **2014**, *15*, 3915–3922. [[CrossRef](#)] [[PubMed](#)]
59. Landarani-Isfahani, A.; Taheri-Kafrani, A.; Amini, M.; Mirkhani, V.; Moghadam, M.; Soozanipour, A.; Razmjou, A. Xylanase immobilized on novel multifunctional hyperbranched polyglycerol-grafted magnetic nanoparticles: An efficient and robust biocatalyst. *Langmuir* **2015**, *31*, 9219–9227. [[CrossRef](#)] [[PubMed](#)]
60. Zivkovic, L.T.; Zivkovic, L.S.; Babic, B.M.; Kokunesoski, M.J.; Jokic, B.M.; Karadzi, I.M. Immobilization of *Candida rugosa* lipase by adsorption onto biosafe meso/macroporous silica and zirconia. *Biochem. Eng. J.* **2015**, *93*, 73–83. [[CrossRef](#)]
61. Calero, J.; Verdugo, C.; Luna, D.; Sancho, E.D.; Luna, C.; Posadillo, A.; Bautista, F.M.; Romero, A.A. Selective ethanolysis of sunflower oil with Lipozyme RM IM, an immobilized *Rhizomucor miehei* lipase, to obtain a biodiesel-like biofuel, which avoids glycerol production through the monoglyceride formation. *New Biotechnol.* **2014**, *31*, 596–601. [[CrossRef](#)] [[PubMed](#)]
62. Dizge, N.; Keskinler, B. Enzymatic production of biodiesel from canola oil using immobilized lipase. *Biomass Bioenergy* **2008**, *32*, 1274–1278. [[CrossRef](#)]
63. Xu, Y.; Nordblad, M.; Nielsen, P.M.; Brask, J.; Woodley, J.M. In situ visualization and effect of glycerol in lipase-catalyzed ethanolysis of rapeseed oil. *J. Mol. Catal. B* **2011**, *72*, 213–219. [[CrossRef](#)]

64. Zdarta, J.; Sałek, K.; Kołodziejczak-Radzimska, A.; Siwińska-Stefańska, K.; Szwarc-Rzepka, K.; Norman, M.; Klapiszewski, Ł.; Bartczak, P.; Kaczorek, E.; Jesionowski, T. Immobilization of *Amano Lipase A* onto Stöber silica surface: Process characterization and kinetic studies. *Open Chem.* **2015**, *13*, 138–148. [[CrossRef](#)]
65. Bradford, M.M. Rapid and sensitive method for the quantitation of microgram quantities of protein utilizing the principle of protein-dye binding. *Anal. Biochem.* **1976**, *72*, 248–254. [[CrossRef](#)]



© 2017 by the authors. Licensee MDPI, Basel, Switzerland. This article is an open access article distributed under the terms and conditions of the Creative Commons Attribution (CC BY) license (<http://creativecommons.org/licenses/by/4.0/>).